Available online at www.sciencedirect.com
SCIENCE DIRECT
International Journal of Heat and Fluid Flow 26 (2005) 914–921
International Journal of HEAT AND FLUID FLOW
www.elsevier.com/locate/ijhff

Droplet combustion experiments in varying forced convection using microgravity environment

Masaki Mitsuya [a], Hironao Hanai [b], Satoru Sakurai [c], Yasuhiro Ogami [c], Hideaki Kobayashi [c,*]

[a] Tokyo Gas Corporation, 1-5-20 Kaigan, Minato-ku, Tokyo 105-0022, Japan
[b] Chiba University of Science, 3 Shiomi-cho, Choshi, Chiba 288-0025, Japan
[c] Institute of Fluid Science, Tohoku University, 2-1-1 Katahira, Aoba-ku, Sendai, Miyagi 980-8577, Japan

Available online 7 November 2005

Abstract

A new microscopic model of the interaction between droplet flames and fine vortex tubes which compose a coherent structure of turbulence was developed. Three non-dimensional numbers were introduced to extend the length scale and time scale so as to be suitable for microgravity experiments using droplets of combustion of about 1 mm in diameter. An experimental apparatus for combustion of a single droplet and that of an array of two droplets in varying airflow was developed, and experiments were performed in microgravity and normal gravity at pressures up to 2.0 MPa for *n*-nonane and ethanol as fuels. Variations of the instantaneous burning rate constant, K_i, in response to the varying flow velocity was successfully observed. At high pressure, the effects of droplet Reynolds number *Re* on K_i was clearly seen, while the effects of natural convection, which increases K_i with *Re*, was seen in normal gravity even in the forced airflows. As for the experiments on combustion of an array of two droplets, K_i reduction of the downstream droplet became weak when the flow direction was varied. However, the K_i reduction of the downstream droplet for flow direction variations was clearly seen for *n*-nonane droplets but almost not for ethanol droplets. The interaction mechanism between upstream and downstream droplets is considered to result from the elimination of oxidizer supply to the downstream droplet, indicating strong interaction effects of *n*-nonane droplets for a stoichiometric oxygen-fuel ratio of *n*-nonane (i.e., 14.0) greater than that of ethanol (i.e., 3.0).

Keywords: Droplet combustion; Forced convection; Microgravity

1. Introduction

Investigation of fundamental phenomenon and modeling of turbulent spray combustion in a high pressure environment is important in terms of development of environmentally low-impact, high-load combustors. However, researches on spray combustion and turbulent flow have been mostly separately performed and those of microscopic interaction of flame and turbulence are very limited (Chiu, 2004).

Recently, a coherent structure of isotropic turbulent flows has been clarified by direct numerical simulation (Vincent and Meneguzzi, 1991). The isotropic turbulence has a structure characterized by many vortex tubes, the diameter of these tubes being several tens to several hundreds of micrometers. The diameters of fuel spray droplets are in a similar size range, so that it is appropriate to assume the existence of interactions between droplet combustion and the vortex tubes, which compose a coherent structure of turbulence.

In this study, we developed a new model of the interaction between droplet flames and vortex tubes which represents the elemental process of turbulent spray combustion shown in Fig. 1. This model focuses on the case in which the droplet diameter is smaller than the vortex tube diameter. When a droplet enters to a vortex flow field represented by the Burgers vortex tube (Kida and Yanagi, 1999), as depicted in the right-hand side of Fig. 1, the

* Corresponding author.
E-mail address: kobayashi@ifs.tohoku.ac.jp (H. Kobayashi).

0142-727X/$ - see front matter © 2005 Elsevier Inc. All rights reserved.
doi:10.1016/j.ijheatfluidflow.2005.10.004

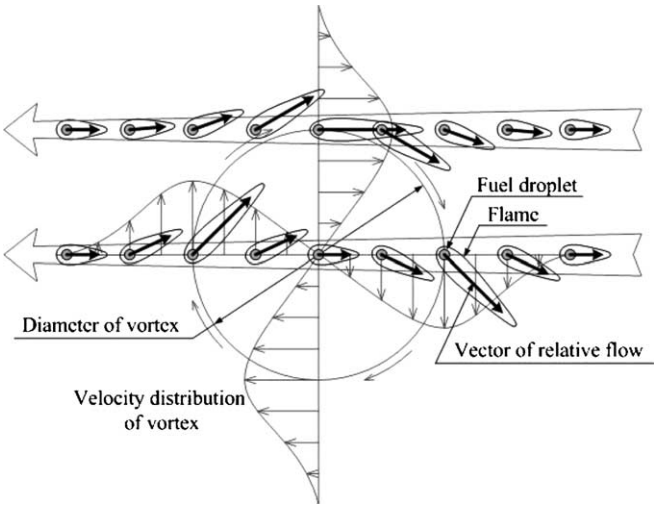

Fig. 1. Proposed model of interaction between droplet combustion and a vortex tube which compose a coherent structure of turbulence.

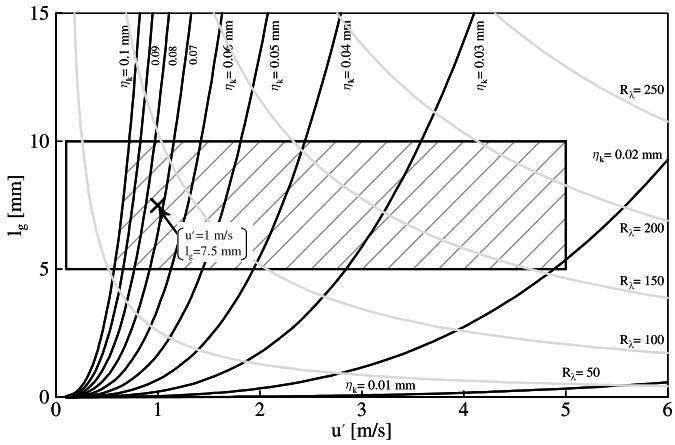

Fig. 2. Range of characteristic values of turbulent flows.

droplet is subjected to variations of the relative flow velocity and relative flow direction. In this study, numerical analysis to estimate flow variations to which a droplet is exposed was performed first and then utilized to design the experimental apparatus. The apparatus was developed to perform both single-droplet experiments and those on an array of two droplets. Microgravity experiments were conducted using the MGLAB drop-shaft facility in the city of Toki, whose free-fall length, duration, and quality of microgravity are 100 m, 4.5 s, and 10^{-5} g, respectively, in order to eliminate the natural convection, especially at high pressure.

2. Analysis and classification of varying forced convection

Prior to the development of the experimental setup and the performance of experiments, numerical analysis of droplet–vortex interaction was performed.

To investigate the interaction between droplet flames and vortex tubes which compose a coherent structure of turbulence, it is necessary to specify turbulent flow characteristics in actual high-load combustors. For ordinary high-load combustors, assumptions of the following range of turbulence parameters are reasonable: 0.1 m/s $< u' <$ 5 m/s, 5 mm $< l_g <$ 10 mm, 0.01 mm $< \eta_k <$ 0.1 mm, and $50 < R_\lambda <$ 250, where u', l_g, η_k, and R_λ are turbulence intensity, integral scale of turbulence, Kolmogorov scale, and turbulence Reynolds number based on Taylor microscale, respectively. When isotropic turbulence is assumed, these four values are not independent and we can obtain their relations as shown in Fig. 2. The shaded area in Fig. 2 corresponds to the range in which the assumed turbulent flow characteristics are taken into account.

Recent direct numerical simulation has revealed that the maximum circumferential flow velocity of a vortex tube, i.e., Burgers vortex tube, is close to u' and that is the vortex diameter is 10–12 times the Kolmogorov scale. The symbol × represents the turbulence characteristics considered for the numerical analysis in this study. The initial droplet diameter and initial velocity of the droplet were assumed to be 50 μm and 2.0 m/s, respectively. When u' and l_g are assumed to be 1.0 m/s and 7.5 mm, as shown in Fig. 2, the maximum circumference flow velocity of the vortex and the vortex diameter can be estimated as 1.0 m/s and 0.872 mm, respectively. The distance from the initial position of the droplet to the vortex center was considered to be twice as large as the vortex diameter, and the initial direction of the droplet is toward the center of the vortex. The motion of the droplet was simulated by solving the momentum equation using the drag coefficient based on Stokes' law and the d^2-low of the droplet diameter for n-decane as a fuel.

Fig. 3 shows an example of calculated results. As can be clearly seen, when the droplet passes through a vortex, it is subjected to both variation of relative flow velocity and flow direction simultaneously.

Although varying relative velocity could be estimated for a 50 μm droplet passing through a vortex tube, it is difficult to perform experiments for such a small droplet. Therefore, when performing our experiments, it was necessary to expand the length scale based on a certain analogy. The following three non-dimensional numbers were introduced to classify the interaction characteristics.

Non-dimensional droplet time

$$\bar{\tau} = \frac{d_0^2 U_0}{Kl}, \tag{1}$$

Initial Reynolds number

$$Re_{\mathrm{drp}} = \frac{d_0 U_0}{\nu}, \tag{2}$$

Oscillation Reynolds number

$$Re_{\mathrm{osc}} = \frac{d_0 u'}{\nu}, \tag{3}$$

where d_0 is the initial droplet diameter, U_0 is the initial droplet velocity, K is the burning velocity constant in

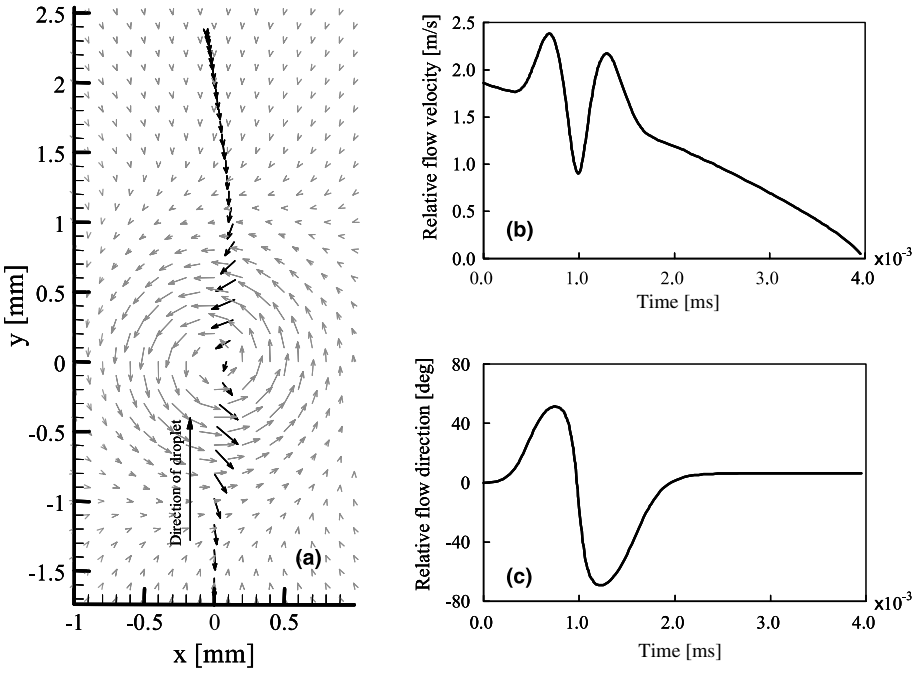

Fig. 3. Calculated droplet motion and varying relative flow: (a) trajectory and relative flow vector, (b) time history of relative flow velocity, and (c) time history of relative flow direction for a single droplet with a diameter of 50 μm.

steady flow, l is the vortex diameter, u' is the turbulence intensity which is the same as the maximum circumferential velocity in the vortex, and ν is the kinematic viscosity.

Non-dimensional droplet time expressed by Eq. (1) is the ratio of droplet lifetime to varying periods. The Reynolds number expressed by Eq. (2) is the droplet Reynolds number in which the initial droplet diameter is used as the characteristic length scale. The Reynolds number expressed by Eq. (3) is the amplitude of varying forced flow using turbulence intensity as the maximum circumference velocity of the vortex. In these three non-dimensional numbers, burning rate constant and initial droplet diameter are included as combustion characteristics, and turbulence intensity and vortex diameter are also included as parameters of turbulent flows.

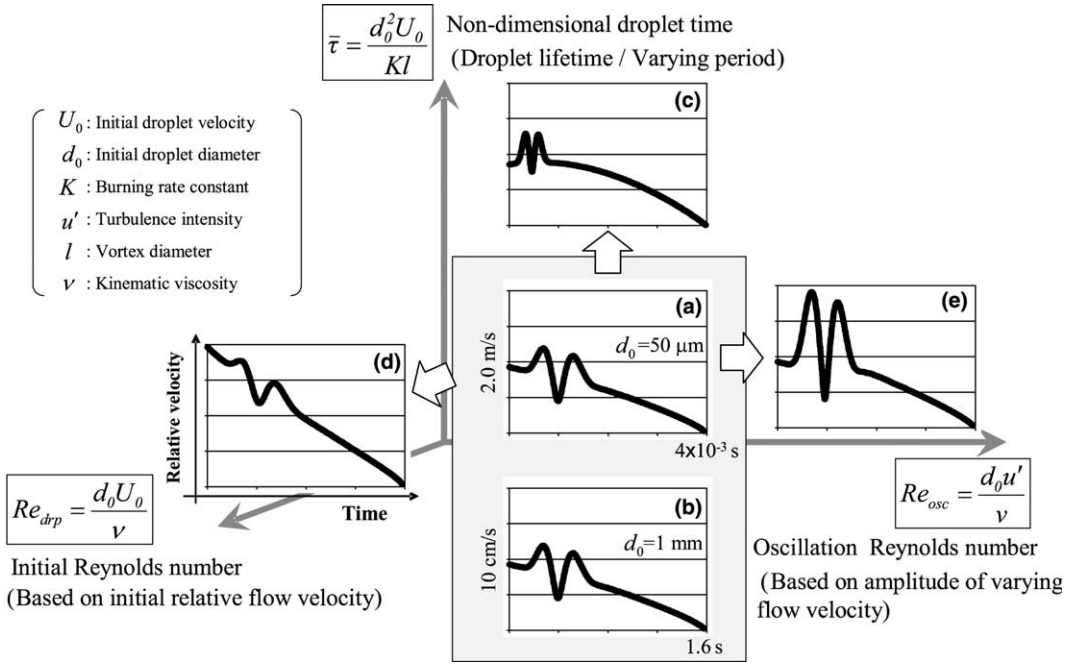

Fig. 4. Characterization of varying relative flow for a burning droplet based on three non-dimensional numbers.

Fig. 4 shows the effects of these three non-dimensional numbers on the patterns of relative flow variations. The flow variation curves in this figure are actual calculated ones. It is seen, for example, that a large $\bar{\tau}$ leads to a small flow variation period and a large Re_{osc} leads to a large amplitude of flow variations. These three non-dimensional numbers mean the droplet–vortex interaction for a small droplet in spray combustion and that for a large droplet in laboratory scale experiments are analogous. As seen in Fig. 4(a) and (b), when these three non-dimensional numbers are kept the same for a small droplet with a diameter of 50 μm and a large droplet with a diameter of 1 mm, the flow variation patterns are possibly the same and combustion duration becomes 1.6 s, which is suitable for microgravity experiments. Based on these findings, we determined the specifications of the experimental apparatus and experimental conditions.

3. Experimental apparatus and procedure

Fig. 5 shows a schematic of the experimental apparatus. A fuel droplet is suspended at the center of the rotary stage using a fine silica fiber with a diameter of 125 ± 10 μm, which has a spherical end 375 ± 25 μm in diameter. Airflow is supplied through a nozzle, whose outlet diameter is 12 mm, mounted on the round plate of the rotary stage driven by a stepping motor. Airflow rate is controlled using a precision needle valve driven by another stepping motor. The cycle and amplitude of the varying airflow rate was confirmed using a hot-wire anemometer. Using this forced convection generator, the flow direction and flow rate of air can be varied for a droplet placed near the nozzle outlet. For the experiments on an array of two droplets, two silica fibers were arranged on the centerline of the air nozzle. The apparatus, including the droplet generator, the forced convection generator, and the igniter, were designed to be small enough to fit in the cylindrical high-pressure chamber with an inner diameter of 109 mm and a length of 500 mm. Observation of the droplet during combustion was performed for back-lit images recorded from the bottom of the suspended droplet using a high-speed video camera, whose frame rate was 500 f/s for single-droplet experiments and 250 f/s for experiments on arrays of two droplets. This apparatus was controlled using a personal computer and LabVIEW-based software developed to follow the sequence of microgravity experiments in MGLAB. This apparatus, including its many components, was installed in a drop capsule and used for both microgravity and normal gravity experiments.

Image processing was conducted to determine the instantaneous burning velocity constant, K_i, defined as the time dependent gradient of the d^2-time history.

n-Nonane (C_9H_{20}) and ethanol (C_2H_5OH) were used as less-volatile and volatile fuels, respectively. The initial droplet diameter was about 1.2 mm and droplet spacing was 2.6 mm for experiments on an array of two droplets.

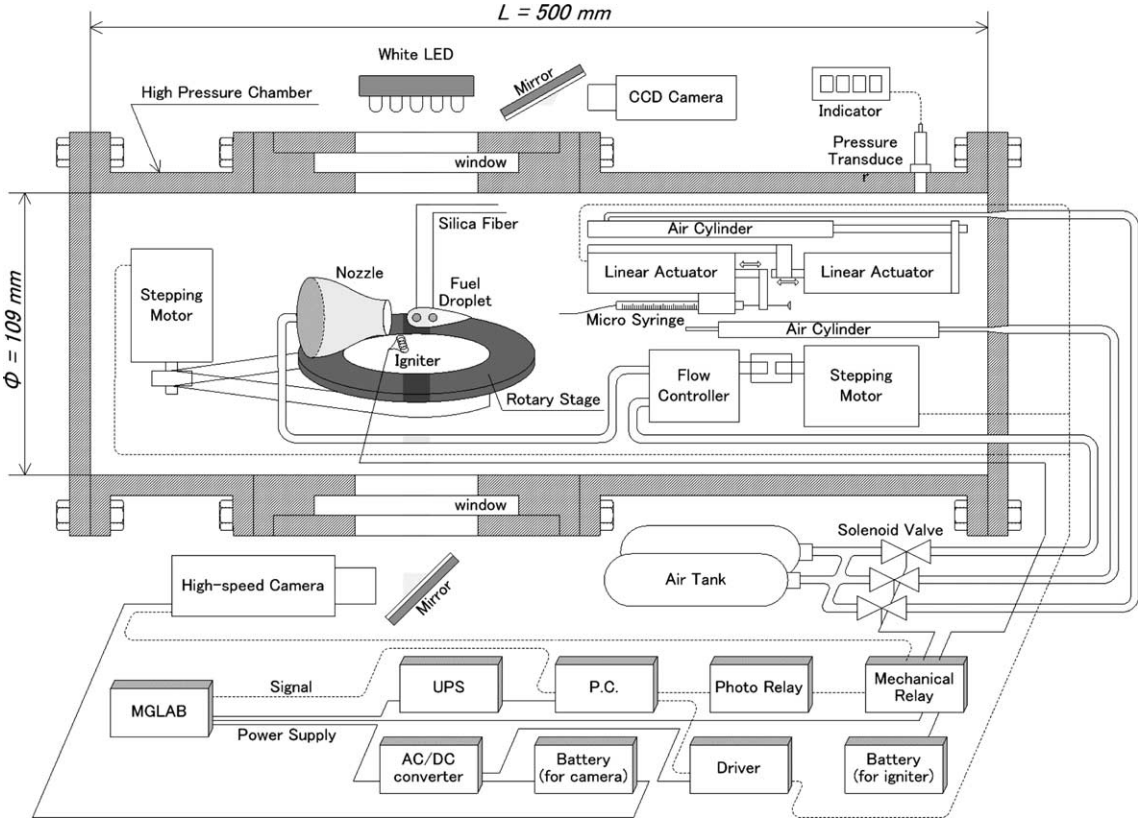

Fig. 5. Schematic of the experimental apparatus.

The maximum pressure in this experiment is 2.0 MPa, which was close to the critical pressure of *n*-nonane.

As mentioned in the previous section, there are many combinations of flow direction, flow velocity, and their cyclic variations. In this study, therefore, in order to investigate the essential effects of varying forced convection on droplet combustion, we focused our the experiments on three cases of flow conditions, i.e., constant flow velocity (CF), flow direction variation without flow velocity variation (VFD), and flow velocity variation without flow direction variation (VFV) for the purpose of comparison.

4. Results and discussion

4.1. Single-droplet combustion

Fig. 6 shows direct photographs of single-droplet flames at various pressures and constant air velocity (CF) of 10 cm/s in microgravity and a normal gravity. In normal gravity, the droplet fell during combustion at pressures over 0.4 MPa due to a decrease in surface tension. Therefore, the pressure range of the experiments in normal gravity had a ceiling of 0.4 MPa. In microgravity, the droplet could be suspended during combustion even at 2.0 MPa. Because of strong light emission from soot, a droplet could not be seen by the naked eye. Using intense back-lit imaging, however, the droplet diameter could be successfully measured. As seen in the photographs in normal gravity, the effect of natural convection is strong, so that the flame downstream tends to be bent in upward.

Fig. 7 shows typical experimental results for a single droplet at 0.1 MPa for a *n*-nonane single droplet in microgravity. The instantaneous burning rate constant, K_i, was determined by calculating the instantaneous gradient of d^2 variations with time, where d is the instantaneous droplet diameter during combustion. Due to the effects of vertical motion of the droplet suspended at the end of the silica fiber, that could not be considered in calculation of the droplet diameter, variation of K_i in the CF case was not smooth. However, it can be clearly seen that the difference in K_i variations in the CF case and the VFD case was very small, while K_i in the VFV case changed periodically with time following the flow velocity variation as shown in Fig. 7(b). The cycle of K_i change well corresponds to the flow velocity cycle in this experiment. The other experimental results, in which the flow velocity was kept at the minimum and maximum velocities of the VFV case of Fig. 7, revealed that the K_i for the VFV case in Fig. 7(a) was between these two values, meaning that the quasi-steady condition of droplet evaporation and combustion in periodically varying air flow was attained. This tendency is similar to the numerical results by Chiu and Huang (1996) for the response of droplet gasification rate in an acoustic oscillation of the oxidizer, while their droplet diameter is much smaller (i.e., 0.1 mm) and frequency of oscillation is much higher (i.e., 2000 Hz). In the VFD case, as seen in Fig. 7, effects of direction change of air flow was not seen clearly. It is presumed that the droplet internal flow (Prakash and Sirignano, 1978) is strong compared to the flow direction change, leading to the uniform temperature

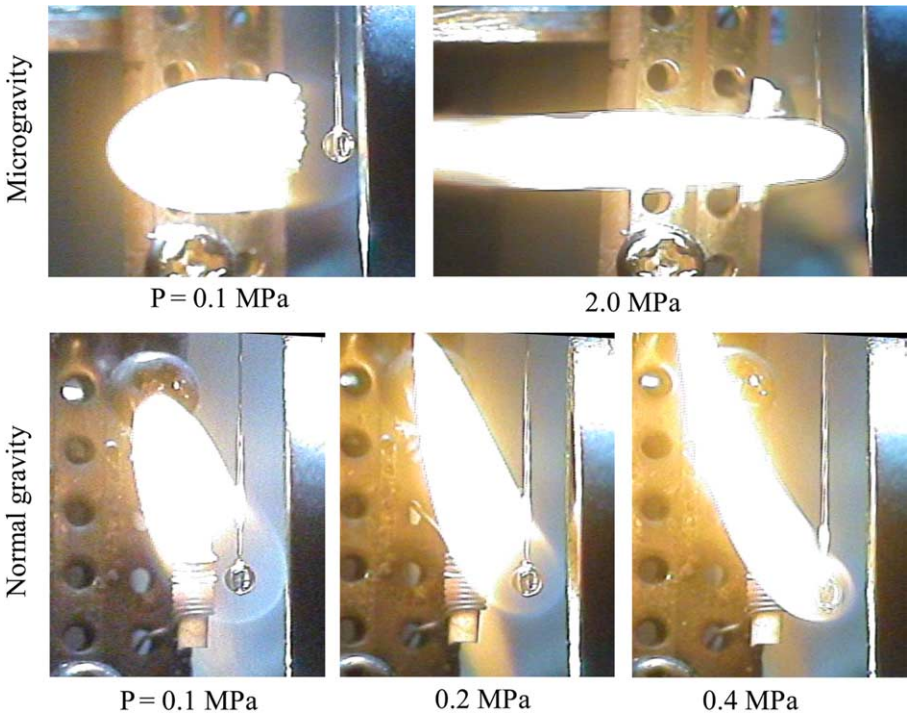

Fig. 6. Direct photographs of single droplet flames at various pressures in microgravity and normal gravity (*n*-nonane, constant flow velocity of $U = 10$ cm/s).

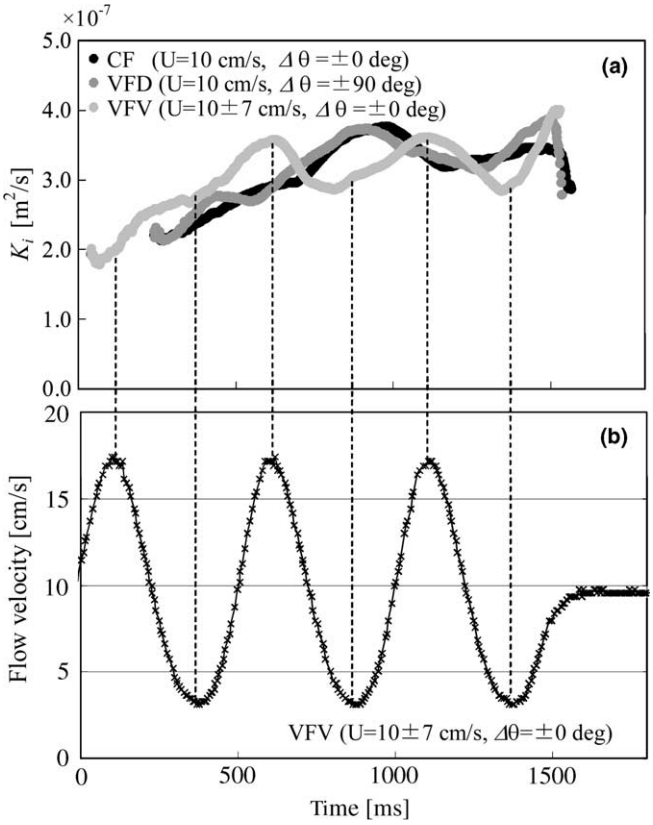

Fig. 7. Time histories of K_i and forced air-velocity variations for *n*-nonane single droplet flames at 0.1 MPa in microgravity: (a) K_i and (b) flow velocity for VFV.

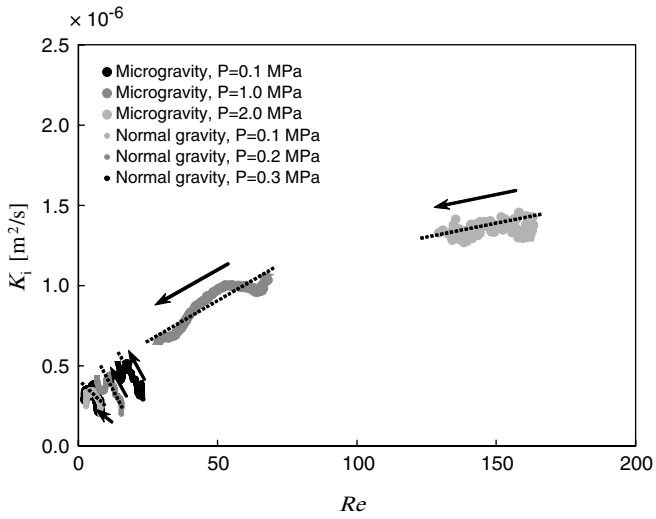

Fig. 8. Effects of pressure on variations of K_i with *Re* during combustion (*n*-nonane, constant flow velocity of $U = 10$ cm/s).

profiles for droplet evaporation. From these experimental results, we can say that effect of flow velocity variation on heat transfer to the droplet surface is significant due to the Reynolds number dependence (Law and Williams, 1972; Ranz and Marshall, 1952), while the flow direction variation effect is small.

Fig. 8 shows the effects of pressure and gravitational conditions on K_i for a *n*-nonane droplet at various pressures in the case of constant air velocity (CF). The abscissa of this figure is the instantaneous droplet Reynolds number, *Re*. The arrows in this figure indicate the direction of the time elapse. It is reasonable to assume that, during the combustion, *Re* decreases because of the decrease in droplet diameter and that K_i also decreases due to the Reynolds number effects (Law and Williams, 1972; Ranz and Marshall, 1952). Chiu and Huang (1996) have reported in their theoretical paper that the transition from envelope flame to wake flame occurs at *Re* of 20–40. However, in our experiments at high pressure, the transition was not seen even though *Re* is over 100.

In normal gravity, however, K_i significantly increases with time. It is supposed that natural convection generates the upward flow even in forced convection and increased airflow velocity near the droplet especially at elevated pressure. In this case, *Re* is the nominal value in terms of the velocity. These results mean that microgravity environments are essential for experiments on droplet combustion, even though forced convection exists.

4.2. Combustion of an array of two droplets

Fig. 9 shows d^2 and K_i variations of the upstream and downstream droplets obtained from experiments on combustion of an array of two droplets in the three cases of CF, VFD, and VFV in microgravity. Two droplets were arranged on the centerline of the air nozzle; the upstream droplet is the one located near the nozzle outlet.

It is seen that the lifetime of the downstream droplet is longer compared with that of the upstream droplet, so that K_i of the downstream droplet is decreased due to the existence of the upstream droplet regardless of airflow variations. If the heating of the downstream droplet by the upstream droplet is effective, the K_i of the downstream droplet should increase. However, the results show that the oxidizer supply is eliminated due to the existence of the upstream droplet flame.

In the VFD case, K_i of the downstream droplet is larger than that of the CF and VFV cases, and thus the lifetime of the downstream droplet is shorter in comparison with the CF and VFV cases. This well corresponds to the mechanism of the decrease in K_i of the downstream droplet and the effects of upstream droplet on the oxidizer supply are predominant for K_i variation of the downstream droplet.

Fig. 10 shows the effects of the kinds of fuel, i.e., *n*-nonane and ethanol, on the interaction in the combustion for varying flow directions (VFD) in microgravity. The ordinate of Fig. 10 is the ratio of instantaneous K_i of the droplet downstream to the K_i of the upstream droplet averaged through the droplet lifetime, meaning that when the K_i ratio is much smaller than unity, the effects of the upstream droplet on combustion of the downstream droplet is

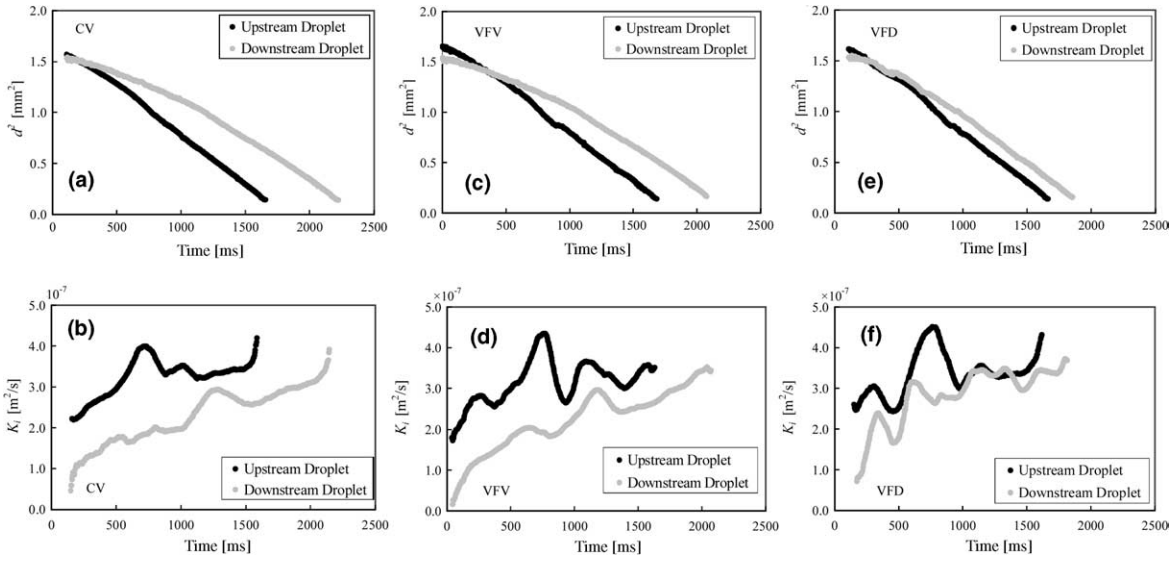

Fig. 9. Time history of d^2 and K_i in experiments on an array of two droplets of *n*-nonane at 0.1 MPa in microgravity: (a) and (b) constant flow velocity, CF ($U = 20$ cm/s, $\Delta\theta = \pm 0°$); (c) and (d) varying flow velocity, VFV ($U = 20 \pm 13$ cm/s, $\Delta\theta = \pm 0°$); (e) and (f) varying flow direction, VFD ($U = 20$ cm/s, $\Delta\theta = \pm 90°$).

strong. We can see that the K_i ratio is smaller than unity at the early stage of combustion and that it increases quickly for *n*-nonane droplets, while the K_i ratio is almost unity over the whole droplet lifetime, indicating that the effects of flow direction variation are more significant for *n*-nonane than for ethanol. As mentioned above, the interaction mechanism between upstream and downstream droplets is considered to be due to the elimination of oxidizer supply to the downstream droplet. Therefore, the strong interaction effects of *n*-nonane droplets are due to the larger stoichiometric oxygen-fuel ratio of *n*-nonane (i.e., 14.0), which is greater than that of ethanol (i.e., 3.0).

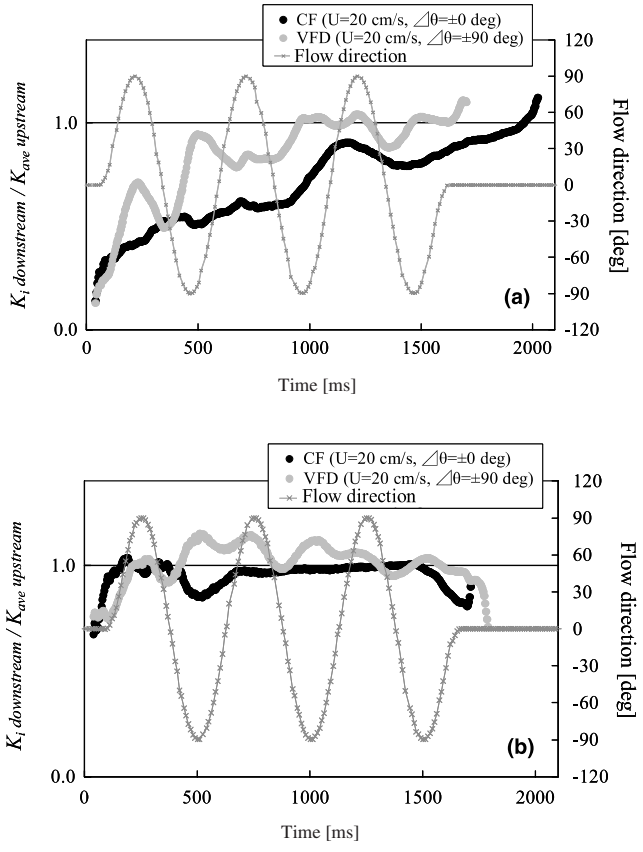

Fig. 10. Time history of K_i *downstream*/K_{ave} *upstream* for an array of two droplets at 0.1 MPa in microgravity: (a) *n*-nonane and (b) ethanol.

These results imply that the varying flow direction caused by turbulence is effective for increasing overall K_i of group combustion (Chiu, 1999) even for liquid fuels with higher molecular weight, and also may give information for more global interaction of droplets evaporation and combustion (Chiu and Su, 1997; Chiu, 2000).

5. Conclusions

A new microscopic interaction model between droplet flames and vortex tubes which compose a coherent structure of turbulence was developed. Based on the model and analysis, an experimental apparatus for combustion of a single droplet and an array of two droplets in varying airflow was developed. Experiments using the apparatus were performed in normal gravity and microgravity and the following results were obtained:

(1) Using three non-dimensional numbers, the flow variation patterns were characterized, and extension of the length scale and time scale could be achieved, leading to suitable conditions of microgravity experiments using droplets having diameters of 1 mm.
(2) As for the experiments on single droplet combustion, variations of the instantaneous burning rate constant, K_i, attributed to varying flow velocity were

successfully obtained. The quasi-steady state of droplet burning regardless of the flow variations was confirmed in the present experimental conditions.

(3) Experimental results at high pressure successfully showed the effects of droplet Reynolds number Re on K_i, while the effects of natural convection, which decreases K_i with Re, was seen, indicating the necessity of conducting microgravity experiments at high pressure.

(4) As for the experiments on combustion of an array of two droplets, the K_i reduction of the droplet downstream became weak when the flow direction was varied, meaning that variation of flow direction caused by turbulence is effective for increasing overall K_i of the group combustion.

(5) The K_i reduction of the droplet downstream, even for flow direction variations, was more significant for *n*-nonane droplets than for ethanol droplets because the stoichiometric oxygen-fuel ratio of the former fuel is larger than that of the latter.

Acknowledgments

The authors would like to express their thanks to Mr. S. Hasegawa for assistance in conducting the experiments. This research was supported by JAXA and the Japan Space Forum, under Ground Research Announcement for Space Utilization.

References

Chiu, H.H., 1999. Advances and challenges in droplets and spray combustion. In: Proceedings of the 2nd Asia–Pacific Conference on Combustion, pp. 54–73.

Chiu, H.H., 2000. Advances in challenges in droplet and spray combustion. I. Towards a unified theory of droplet aerothermochemistry. Progress in Energy and Combustion Science 26, 381–416.

Chiu, H.H., 2004. Modeling liquid-propellant spray combustion processes. In: Yang, V. (Ed.), Liquid Rocket Thrust Chamber: Aspects of Modeling, Analysis, and Design, Progress in Aeronautics and Astronautics, vol. 200, pp. 251–293.

Chiu, H.H., Huang, J.S., 1996. Multiple-state phenomena and hysteresis of a combusting isolated droplet. Atomization and Sprays 6, 1–26.

Chiu, H.H., Su, S.P., 1997. Theory of droplets (II): states, structures, and laws of interacting droplets. Atomization and Sprays 7, 1–32.

Kida, S., Yanagi, S., 1999. Dynamics of Turbulent Flows. Asakura-shoten, Tokyo (in Japanese).

Law, C.K., Williams, F.A., 1972. Kinetics and convection in the combustion of alkane droplets. Combustion and Flame 19, 393–405.

Prakash, S., Sirignano, W.A., 1978. Liquid droplet heating with internal circulation. International Journal of Heat and Mass Transfer 21, 885–895.

Ranz, W.E., Marshall Jr., W.R., 1952. Evaporation from drops. Chemical Engineering Progress 48, 141–146, 173–180.

Vincent, A., Meneguzzi, M., 1991. The spatial structure and statistical properties of homogeneous turbulence. Journal of Fluid Mechanics 225, 1–20.